

Understanding Oversquashing in GNNs through the Lens of Effective Resistance

Mitchell Black ^{*} Amir Nayyeri [†] Zhengchao Wan [‡] Yusu Wang [§]

Abstract

Message passing graph neural networks are popular learning architectures for graph-structured data. However, it can be challenging for them to capture long range interactions in graphs. One of the potential reasons is the so-called oversquashing problem, first termed in [Alon and Yahav, 2020], that has recently received significant attention. In this paper, we analyze the oversquashing problem through the lens of *effective resistance* between nodes in the input graphs. The concept of effective resistance intuitively captures the “strength” of connection between two nodes by paths in the graph, and has a rich literature connecting spectral graph theory and circuit networks theory. We propose the use the concept of *total effective resistance* as a measure to quantify the total amount of oversquashing in a graph, and provide theoretical justification of its use. We further develop algorithms to identify edges to be added to an input graph so as to minimize the total effective resistance, thereby alleviating the oversquashing problem when using GNNs. We provide empirical evidence of the effectiveness of our total effective resistance based rewiring strategies.

1 Introduction

Graph neural networks (GNNs) are powerful tools for graph learning and optimization tasks [Scarselli et al., 2008]. One major framework for GNNs is *message passing*, where node/edge features are repeatedly aggregated locally through node neighborhoods. The number of layers of GNNs intuitively corresponds to the radius of the neighborhood of a graph node where the information aggregation will happen. When the number of layers is small, the message passing will be done locally, and the GNN will not be able to capture information from long-range interactions, a problem known as *underreaching*. On the other hand, choosing a large number of layers can lead to *oversmoothing*, where features might be smoothed out and become indistinguishable [Cai and Wang, 2020, Oono and Suzuki, 2020]. A third issue is *oversquashing* [Alon and Yahav, 2020], where as larger neighborhoods are considered, information from long-range interactions passing through certain “bottlenecks” of the underlying graph will have negligible impact on the training of GNNs. This behaviour was named oversquashing as information from potentially exponentially many (with respect to the number of layers) nodes will be squashed into node vectors.

Recently, the oversquashing problem has been analyzed through different techniques such as graph curvature [Topping et al., 2021] and information theory [Banerjee et al., 2022]. Moreover, different *rewiring techniques* have been proposed to alleviate oversquashing, where the graph structures is altered to decrease bottlenecks in the graph before applying GNNs [Deac et al., 2022, Karhadkar et al., 2022].

In this paper, we propose to analyze the oversquashing problem through the lens of *effective resistance*. Effective resistance originates from Electrical Engineering [Kirchhoff, 1847], where the effective resistance between two nodes u and v in an electrical network is the difference in voltage between u and v when a unit of current is inserted at u and removed at v . Since then, effective resistance has taken on a new life in Graph Theory, where effective resistance has been shown to be tied to many properties of the graph underlying the electrical network [Doyle and Snell, 1984, Lyons and Peres, 2017]. For example, the effective resistance between a pair of vertices is proportional to the *commute time* between two vertices—the expected

^{*}School of Electrical Engineering and Computer Science, Oregon State University: blackmit@oregonstate.edu

[†]School of Electrical Engineering and Computer Science, Oregon State University: nayyeria@oregonstate.edu

[‡]Halıcıoğlu Data Science Institute, University of California San Diego: zcwan@ucsd.edu

[§]Halıcıoğlu Data Science Institute, University of California San Diego: yusuwang@ucsd.edu

number of steps in a random walk from one vertex to the other and back [Chandra et al., 1996]. The effective resistance between the end points of an edge is proportional to the probability of the edge being included in a random spanning tree of the graph [Biggs, 1997]. Furthermore, the effective resistance is closely related to the Cheeger constant for graphs that measures bottlenecks in graphs [Mémoli et al., 2022]. With its various connections to many other objects (e.g., random walks and Laplace operators), effective resistance has been widely used in practice; e.g., [Spielman and Srivastava, 2011, Alev et al., 2018, Ahmad et al., 2021].

These properties suggest that the effective resistance is a measure of “well-connectedness” between graph nodes (see more discussions in Section 3). In this paper, we will show that the effective resistance can also be used to quantify oversquashing behavior in graph neural networks. In particular, the lower the effective resistance between a pair of node is, the less oversquashing is experienced by a graph neural network sending messages between these nodes.

Main contributions. In this paper, we propose to use effective resistance as a way to quantify oversquashing in graph neural networks. We further study how this can be used to modify input graphs to alleviate the oversquashing problem.

- In Section 3, we prove that the information passed from one node to another by any number of layers of a GNN is upper bounded by a quantity related to the effective resistance between the nodes.
- In Section 4, we utilize total effective resistance as a global measure of oversquashing and develop a rewiring algorithm for minimizing total effective resistance by adding edges to the graphs.
- In Section 5, we empirically demonstrate that our rewiring technique is effective in alleviating the oversquashing problem. Our method outperforms the curvature based method SDRF from [Topping et al., 2021] and has similar performance compared to the spectral gap based method FoSR from [Karhadkar et al., 2022].

All missing technical details and proofs are in the Appendix.

More on related work. [Topping et al., 2021] were the first to introduce a method for quantitatively analyzing the oversquashing problem. They proposed the norm of the Jacobian between node features at different levels of a GNN as a measure of oversquashing, as the norm of the Jacobian represents the ability of the features at one node to influence the features at another. They proved an upper bound on the norm of the Jacobian for certain nodes by the Balanced Forman Curvature of an edge. They also proposed a rewiring technique to alleviate the oversquashing problem by increasing the curvature of edges in the graph, mimicking the continuous process of Ricci flow on manifolds. However, their theoretical analysis has the limitation that their final upper bound of Jacobian matrices via curvature only applies to nodes within 2-hop neighborhoods. In contrast, our analysis (Lemma 2 and Theorem 1) applies to any two nodes at any layer of the GNN.

[Banerjee et al., 2022] proposed an approach for analyzing the oversquashing problem using techniques from information theory and a rewiring method targeted at edges with high effective resistance. Although their rewiring algorithms targets edges with high effective resistance, their theoretical analysis does not connect the problem of oversquashing to effective resistance. Furthermore, while both are based on targeting high effective resistance, their rewiring approach is quite different from ours: their approach only involves flipping existing edges randomly with a probability proportional to edge effective resistance, whereas our approach rewrites the graph by considering effective resistances of all pairs of vertices (including those that are not edges).

In their follow-up work, [Karhadkar et al., 2022] introduced another rewiring algorithm aimed at minimizing the spectral gap of the graph, which is related to bottlenecks of graphs through the Cheeger inequality [Chung, 1996]. They also proposed to apply relational GNNs (R-GNNs) [Battaglia et al., 2018] to incorporate structural information from both the original graphs and the graphs after rewiring. Our rewiring technique share a similar framework as theirs: we add edges that minimize the total effective resistance the most and use R-GNNs so that one can treat newly added edges differently from the original edges. Conceptually speaking, however, our approach may lead to better results as the total effective resistance reflects the entire spectrum of the graph Laplacian, including the spectral gap. See our discussion in Section 3.2.

2 Background

This section reviews some definitions from spectral graph theory; see books by Chung [Chung, 1997] and Spielman [Spielman, 2019] for a more thorough introduction.

2.1 Matrices and Spectra of Graphs.

Let $G = (V, E)$ be a connected, undirected, unweighted graph with n vertices and m edges. Let A be the **adjacency matrix** and D be the **degree matrix**. Then $L = D - A$ is the **Laplacian**. Additionally, let $\hat{A} = D^{-1/2}AD^{-1/2}$ be the **normalized adjacency matrix** and $\hat{L} = I - \hat{A} = D^{-1/2}LD^{-1/2}$ be the **normalized Laplacian**.

The matrices \hat{L} and \hat{A} have the same orthonormal basis of eigenvectors $\{z_i : 1 \leq i \leq n\}$ (up to choice of basis) but different eigenvalues. The eigenvalues λ_i of \hat{L} are in the range $[0, 2]$, and the eigenvalues of \hat{A} are $\mu_i = 1 - \lambda_i$, which are in the range $[-1, 1]$. The matrix \hat{A} always has eigenvalue 1 and has eigenvalue -1 if and only if G is bipartite. We use the notational convention that $\lambda_n \geq \dots \geq \lambda_2 > \lambda_1 = 0$ and $\mu_n \leq \dots \leq \mu_2 < \mu_1 = 1$. z_1 , the μ_1 -eigenvector of \hat{A} satisfies $z_1(v) = \sqrt{d_v/2m}$, where d_v is the degree of a vertex v .

2.2 Graph Neural Networks

Consider a graph G with node features $X \in \mathbb{R}^{n \times d}$. We let $x_v \in \mathbb{R}^d$ denote the row in X corresponding to the vertex $v \in V$. A **Graph Neural Network** (GNN) updates the node features by iteratively aggregating features of node in the neighborhood. More precisely, the feature vectors at each layer are computed by

$$h_v^{(0)} := x_v, \quad h_v^{(l+1)} = \phi_l \left(h_v^{(l)}, \sum_{u \in \mathcal{N}(v)} \hat{A}_{uv} \psi_l \left(h_u^{(l)} \right) \right)$$

for learnable functions ϕ_l and ψ_l .

Relational GNNs. In the process of graph rewiring, the structure of the underlying graph will be changed. In order to retain information of the original graph and also exploit the new graph structure induced from graph rewiring, we use **relational GNNs** (R-GNNs) [Battaglia et al., 2018] to accommodate both information. The idea of using R-GNNs for rewired graphs was introduced in [Karthadkar et al., 2022]. In the framework of R-GNNs, for a graph G , there exists a set \mathcal{R} of relation types such that each edge $\{u, v\} \in E$ is associated with an edge type $r \in \mathcal{R}$. We say this edge $\{u, v\}$ of type r . For each $v \in V$ and $r \in \mathcal{R}$, we let $\mathcal{N}_r(v) \subseteq \mathcal{N}(v)$ denote the collection of all neighbors of v incident to an edge of type r . Then, a R-GNN is of the following form

$$h_v^{(l+1)} = \phi_l \left(h_v^{(l)}, \sum_{r \in \mathcal{R}} \sum_{j \in \mathcal{N}_r(v)} \hat{A}_{uv} \psi_l^r \left(h_u^{(l)} \right) \right)$$

for learnable functions ϕ_l and ψ_l^r .

3 Effective Resistance and Oversquashing

Let u and v be vertices of G . The **effective resistance** between u and v is defined

$$R_{u,v} = (1_u - 1_v)^T L^+ (1_u - 1_v),$$

where 1_v is the indicator vector of the vertex v and L^+ is the pseudoinverse of L . The effective resistance can also be computed using the normalized Laplacian \hat{L} as follows.

Lemma 1. *Let G be a connected graph. Let u and v be two vertices. Then,*

$$R_{u,v} = \left(\frac{1}{\sqrt{d_u}} 1_u - \frac{1}{\sqrt{d_v}} 1_v \right)^T \hat{L}^+ \left(\frac{1}{\sqrt{d_u}} 1_u - \frac{1}{\sqrt{d_v}} 1_v \right).$$

This formula for effective resistance is non-standard, and we provide a proof of its correctness in Appendix A.1.

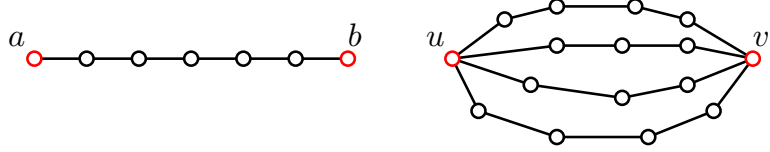


Figure 1: Two examples where the effective resistances can be easily determined. Left: For path graphs, $R_{a,b}$ is just the length of the path; thus $R_{a,b} = 6$. Right: For the vertices u and v connected by several vertex-disjoint paths, $R_{u,v} = (\sum_{\text{path } \ell \text{ connecting } u \text{ and } v} \text{length}(\ell)^{-1})^{-1}$; thus $R_{u,v} = 10/9$.

Intuitively, the effective resistance is a measure of how “well-connected” two vertices u and v are. While the notion of “well-connected”-ness is informal, there are many theorems which suggest such a connection. For example, if u and v are connected by k edge-disjoint paths of length at most l , then the effective resistance $R_{u,v}$ is at most l/k . Therefore, the more and shorter paths connecting u and v , the smaller the effective resistance between u and v . See the introduction for more intuition behind effective resistance.

3.1 Effective Resistance and the Jacobian of GNNs.

As a way of measuring oversquashing in graph neural networks, [Topping et al., 2021] proposed upper bounding the 2-norm of the Jacobian between node features $\left\| \frac{\partial h_u^{(r)}}{\partial x_v} \right\|$ (here both $h_u^{(r)}$ and x_v are vectors and hence $\frac{\partial h_u^{(r)}}{\partial x_v}$ should be understood as a Jacobian matrix instead of just a partial derivative), which captures the influence of initial feature vector x_v at vertex v upon the feature vector $h_u^{(r)}$ at vertex u at the r -th layer of the GNN. A smaller upper bound on the partial derivative indicates that the features at one node can have less influence on the node features at another node. We adopt this way of analysis and establish a bound for the Jacobian matrix via the effective resistance.

First of all, we show how the Jacobian is upper bounded by the power of the normalized adjacent matrix \hat{A} .

Lemma 2. *Let $u, v \in V$ and let $r \in \mathbb{N}$. Assume that $\|\nabla \phi_l\| \leq \alpha$ and $\max\{\|\nabla \psi_l\|, 1\} \leq \beta$ for all $l = 0, \dots, r$, where ∇f denotes the Jacobian of a map f . Then,*

$$\left\| \frac{\partial h_u^{(r)}}{\partial x_v} \right\| \leq (2\alpha\beta)^r \sum_{l=0}^r (\hat{A}^l)_{uv}.$$

This result is different from Lemma 1 in [Topping et al., 2021] in which the two vertices u and v are required to be exactly distance r apart from each other; while our result is for any two vertices.

We can now use this bound to establish a new bound via effective resistance. Recall that $\mu_n \leq \dots \leq \mu_2 < \mu_1 = 1$ denote the eigenvalues of \hat{A} . Then,

Theorem 1. *Let G be a non-bipartite graph. Let $u, v \in V$. Let $\|\nabla \phi_l\| \leq \alpha$ and $\max\{\|\nabla \psi_l\|, 1\} \leq \beta$. Let $d_{\min} = \min\{d_u, d_v\}$ and $d_{\max} = \max\{d_u, d_v\}$. Let $\max\{|\mu_2|, |\mu_n|\} \leq \mu$. Then,*

$$\left\| \frac{\partial h_u^{(r)}}{\partial x_v} \right\| \leq (2\alpha\beta)^r \cdot \frac{d_{\max}}{2} \cdot \left(\frac{2}{d_{\min}} \left(2r + \frac{\mu^{r+1}}{1-\mu} \right) - R_{u,v} \right).$$

Theorem 1 intuitively suggests that vertices with low effective resistance have a better influence over each other in message passing; that is, the node feature $h_u^{(r)}$ at node u in level r is more affected by the initial node feature x_v at node v . Intuitively this makes sense, as effective resistance is tied to the number and length of paths connecting u and v . The more and shorter paths connecting u and v , the lower the effective resistance between u and v is. This implies that there are more ways for a graph neural network to send messages between u and v and indeed, by Theorem 1, the less oversquashing between u and v .

Sketch of proof of Theorem 1. The proof of Theorem 1 is based on the following two lemmas, which themselves may be of independent interest. Detailed proofs of the theorem and the lemmas can be found in Appendix A.3.

We let \hat{A}_r denote the restriction of \hat{A} to the space orthogonal to the eigenvector z_1 , i.e. $\hat{A}_r = \sum_{i=2}^n \mu_i z_i z_i^T$. Recall that the eigenvalues of \hat{A} are in the range $[-1, 1]$, or $(-1, 1)$ if \hat{A}_r is not bipartite. Then, the pseudoinverse of \hat{L} can be characterized as follows.

Lemma 3. *Let G be a connected, non-bipartite graph. Then $\hat{L}^+ = \sum_{j=0}^{\infty} \hat{A}_r^j$.*

This novel characterization of \hat{L}^+ gives rise to the following relationship between the effective resistance and the normalized adjacency matrix \hat{A} .

Lemma 4. *Let G be a non-bipartite graph. Let u and v be two vertices in G . Then,*

$$R_{u,v} = \sum_{i=0}^{\infty} \left(\frac{1}{d_u} (\hat{A}^i)_{uu} + \frac{1}{d_v} (\hat{A}^i)_{vv} - \frac{2}{\sqrt{d_v d_u}} (\hat{A}^i)_{uv} \right).$$

Then, the upper bound in Theorem 1 follows from Lemma 2 and Lemma 4. \square

We now take our analysis one step further and summarize message passing rate between **all pairs** of nodes at any given layer of GNN using the notion of **total effective resistance** R_{tot} —the sum of the effective resistance between all pairs of vertices. As the partial derivative between a pair of vertices is bounded above by a function of the effective resistance, the total resistance can be seen as a measure of oversquashing between all pairs of vertices in the graph. The following corollary follows immediately from Theorem 1 and shows that total resistance can be used as a measure for total oversquashing in a graph.

Corollary 1. *Let G be a non-bipartite graph. Let $\|\nabla \phi_l\| \leq \alpha$ and $\max\{\|\nabla \psi_l\|, 1\} \leq \beta$. Let $d_{\min} = \min_{v \in V} d_v$ and $d_{\max} = \max_{v \in V} d_v$. Let $\max\{|\mu_2|, |\mu_n|\} \leq \mu$. Then*

$$\begin{aligned} & \sum_{u \neq v \in V} \left\| \frac{\partial h_u^{(r)}}{\partial x_v} \right\| \\ & \leq (2\alpha\beta)^r \frac{d_{\max}}{2} \left(\frac{n \cdot (n-1)}{d_{\min}} \left(2r + \frac{\mu^{r+1}}{1-\mu} \right) - R_{\text{tot}} \right). \end{aligned}$$

Comparison with Curvature Bounds. Theorem 1 and Corollary 1 are inspired by Theorem 4 in [Topping et al., 2021], which bounds the Jacobian matrix between vertex features by the Balanced Forman curvature of an edge. In some ways, effective resistance and Balanced Forman curvature are similar, as both measure how connected the endpoints are. However, our analysis generalizes the previous bound in several important ways.

- (1) Our analysis can be applied to any pair of vertices in a graph, not just those vertices at distance 2.
- (2) Effective resistance can be used to measure the oversquashing between vertex features after an arbitrary number of layers of a graph neural network, unlike Balanced Forman Curvature which can only measure oversquashing for 2 consecutive layers of a GNN.

In short, the reason for both of these generalizations is that effective resistance measures the *global* connectivity between a pair of vertices, while Balanced Forman curvature only measures the local connectivity between a pair of nodes. See Figure 2 for an illustration.

3.2 Effective Resistance and the Spectral Gap

Let $0 = \sigma_1 \leq \sigma_2 \leq \dots \leq \sigma_n$ denote the eigenvalues of the (un-normalized) Laplacian L . The second eigenvalue σ_2 is called the **spectral gap**¹ of the graph G . The spectral gap is often used as a measure of “bottleneck” of a graph. This is because the spectral gap is related to the size of the sparsest cut in the graph, a classic result known as **Cheeger’s Inequality** [Chung, 1996].

¹In this section, we focus on the spectral gap and eigenvalues of the *unnormalized* Laplacian, while previous papers studying oversquashing have focused on the spectral gap of the *normalized* Laplacian. There are variants of Cheeger’s inequality for both the normalized and unnormalized spectral gap [Chung, 1997], so both spectral gaps provide a measure of the connectivity and bottleneck of a graph. Generally, the eigenvalues of L and \hat{L} are closely related as follows: $d_{\min} \lambda_k \leq \sigma_k \leq d_{\max} \lambda_k$.

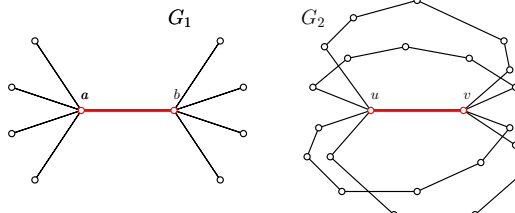


Figure 2: The edges $\{a, b\}$ and $\{u, v\}$ have the same Balanced Forman curvature of $\text{Ric}(a, b) = \text{Ric}(u, v) - 6/5$. However, their effective resistance are different ($R_{a,b} = 1$ and $R_{u,v} = 3/5$). This shows how the curvature only measure local connectivity and does not distinguish global connectivity as effective resistance does.

Previous research on understanding oversquashing has attempted to connect oversquashing to the spectral gap of the graph [Topping et al., 2021, Banerjee et al., 2022]. This has motivated rewiring heuristics aimed at raising at the spectral gap [Banerjee et al., 2022, Deac et al., 2022, Karhadkar et al., 2022]. However, unlike our theoretical analysis for effective resistance (Theorem 1 and Corollary 1), while the use of spectral gap for addressing the oversquashing issue is intuitive, there is no theoretical justification yet for how the spectral gap is directly bounding information passing between nodes.

In this section, we will first provide some discussions on connections between spectral gap and effective resistance in order to derive a first step theoretical justification for using spectral gap for oversquashing. Then, we discuss potential limitations of using only spectral gap for oversquashing.

First of all, the following existing result shows that the worst-case effective resistance between any pair of nodes is proportional to the spectral gap.

Theorem 2 (Theorem 4.2, [Chandra et al., 1996]). *Let R_{\max} denote the maximum effective resistance between any pair of vertices in G . Then,*

$$\frac{1}{n\sigma_2} \leq R_{\max} \leq \frac{2}{\sigma_2}.$$

The above result shows that the worst case oversquashing between a pair of vertices is tied to the spectral gap. Theorem 2 therefore reinforces the idea that low spectral gap is tied to oversquashing. More specifically, as a direct consequence of Corollary 1, one has that

Corollary 2. *Under the same assumptions as in Corollary 1, one has that*

$$\begin{aligned} & \sum_{u \neq v \in V} \left\| \frac{\partial h_u^{(r)}}{\partial x_v} \right\| \\ & \leq (2\alpha\beta)^r \frac{d_{\max}}{2} \left(\frac{n \cdot (n-1)}{d_{\min}} \left(2r + \frac{\mu^{r+1}}{1-\mu} \right) - \frac{1}{n\sigma_2} \right). \end{aligned}$$

Of course, the bound above is looser than the one using R_{tot} in Corollary 1. Furthermore, the following result suggests that that oversquashing behavior of the entire graph is tied not just to the spectral gap, but rather to the *entire* spectrum of the Laplacian. Therefore, raising the entire spectrum of the Laplacian, not just the spectral gap, could potentially further reduce oversquashing in the entire network.

Theorem 3 (Section 2.5, Ghosh et al. [Ghosh et al., 2008]). *Let G be a connected graph with n vertices, Laplacian L , and total resistance R_{tot} . Then*

$$R_{\text{tot}} = n \cdot \text{tr } L^+ = n \cdot \sum_{i=2}^n \frac{1}{\sigma_i}$$

The higher eigenvalues of L also carry topological meaning for the graph. Just as the spectral gap λ_2 measures the obstruction to bipartitioning a graph (the "bottleneck"), λ_k is related to partitioning a graph into k parts [Lee et al., 2014]. See footnote for relationship between λ_k and σ_k .

4 Minimizing Total Resistance by Rewiring

Motivated by Corollary 1, we propose to address oversquashing by “rewiring” a graph to minimize its total resistance. Adding any edge to the graph will decrease its total resistance (a result known as **Rayleigh Monotonicity**), so in this section, we (1) derive a formula to determine how much adding a specific edge decreases the total resistance and (2) propose a rewiring method by greedily adding edges to graphs. Note that our “rewiring” just refers to adding new edges, while some previous usage of the term “rewiring” might refer to replacing one edge with another [Topping et al., 2021, Banerjee et al., 2022].

Change of R_{tot} after adding one edge. We first need a new notion. The **biharmonic distance** between a pair of vertices u and v is

$$B_{u,v} = (1_u - 1_v)^T (L^+)^2 (1_u - 1_v).$$

The biharmonic distance was first introduced in the context of geometry processing [Lipman et al., 2010]. However, before it was properly named, it was discovered that the biharmonic distance between u and v is proportional to the partial derivative of the total resistance with respect to the weight of the edge $\{u, v\}$, i.e. $\partial R_{\text{tot}} / \partial w_{u,v} = -n \cdot B_{u,v}$ [Ghosh et al., 2008]. This suggests that the biharmonic distance can be used as a measure for the effect an edge has on the global connectivity of the graph.

The following theorem may be seen as the unweighted and combinatorial analogue of the previous result (but is proved using completely different means.) This theorem allows us to calculate how much the total resistance decreases when an (unweighted) edge $\{u, v\}$ is added to the graph.

Theorem 4. *Let G be a connected graph with n vertices. Let $\{u, v\}$ be an edge not in G . The difference in total resistance after adding the edge $\{u, v\}$ to G is*

$$R_{\text{tot}}(G) - R_{\text{tot}}(G \cup \{u, v\}) = n \cdot \frac{B_{u,v}}{1 + R_{u,v}}$$

Sketch of proof of Theorem 4. Note that adding the edge $\{u, v\}$ to G changes the Laplacian from L to $L + (1_u - 1_v)(1_u - 1_v)^T$. Hence by Theorem 3 we need to compare the traces of the pseudoinverses of L and $L + (1_u - 1_v)(1_u - 1_v)^T$. This naturally leads us to apply Woodbury’s formula:

Lemma 5 (Woodbury’s Formula). *Let A be an invertible matrix. Let x be a vector. Then*

$$(A + xx^T)^{-1} = A^{-1} - A^{-1}x(1 + x^T A^{-1}x)^{-1}x^T A^{-1}.$$

As L is singular, one cannot apply Woodbury’s Formula directly to $L + (1_u - 1_v)(1_u - 1_v)^T$. Hence, we consider the variant of the Laplacian $L + \frac{11^T}{n}$, where 1 is the all-ones vector. If G is connected, then $L + \frac{11^T}{n}$ is invertible. Moreover, we can show that

Lemma 6. *Let G be a connect graph. Then,*

- $R_{u,v} = (1_u - 1_v)^T (L + \frac{11^T}{n})^{-1} (1_u - 1_v);$
- $B_{u,v} = (1_u - 1_v)^T (L + \frac{11^T}{n})^{-2} (1_u - 1_v);$
- $R_{\text{tot}} = n \cdot \text{tr}(L + \frac{11^T}{n})^{-1} - n.$

One can therefore apply Lemma 5 for computing $(L + \frac{11^T}{n} + (1_u - 1_v)(1_u - 1_v)^T)^{-1}$, take the trace, and conclude the proof. See Appendix A.4 for all the details. \square

Rewiring heuristic. Motivated by Theorem 4, we propose the following heuristic, called ***Greedy Total Resistance (GTR) rewiring***, to minimize the total resistance: repeatedly add the edge $\{u, v\}$ that maximizes $B_{u,v}/(1+R_{u,v})$. For disconnected graphs, the effective resistance and biharmonic distance between vertices in different components is not meaningful. Therefore, in this paper, we only add edges between vertices that are already in the same connected component. While we could also use Theorem 4 to determine which edge to remove to most decrease the total resistance, we will only add edges in this paper.

Time complexity. The time complexity for GTR rewiring depends on the time it takes to (step 1) compute the effective resistance and biharmonic distance for each pair of vertices, (step 2) find the pair of vertices maximizing $R_{u,v}/(1+B_{u,v})$, and (step 3) update the effective resistance and biharmonic distance. If we are adding k edges to the graph, the naive implementation for GTR takes $O(n^3 + kn^2)$ time. We can compute L^+ and L^{2+} in $O(n^3)$ time using the singular value decomposition, which we can use to compute all pairs effective resistance and biharmonic distance in time $O(n^2)$. In total, step (1) would take $O(n^3 + n^2)$ time. Step (2) would take $O(n^2)$ time to iterate over all pairs of vertices. Finally, for step (3), we can update L^+ and L^{2+} in $O(n^2)$ time. This is because adding the edge $\{u, v\}$ to G only causes a constant-rank change to the Laplacian; the Laplacian changes from L to $L + (1_u - 1_v)(1_u - 1_v)^T$ and the squared Laplacian changes from L^2 to $L^2 + L(1_u - 1_v)(1_u - 1_v)^T + (1_u - 1_v)(1_u - 1_v)^T L + (1_u - 1_v)(1_u - 1_v)^T$. The pseudoinverse of L^+ and L^{2+} can then be updated in $O(n^2)$ using Woodbury's Formula (see Lemma 5).

However, more efficient implementations for GTR are possible thanks to nearly-linear time Laplacian solvers: algorithms for solving linear systems of the form $Lx = b$ in $O(m \text{ poly log } n)$ time [Spielman and Teng, 2004, Jambulapati and Sidford, 2021]. Using these algorithms, the pseudoinverses L^+ and L^{2+} could be computed in $O(n \cdot m \text{ poly log } n)$ by using Laplacian solvers to find the columns of the matrix. Alternatively, all-pairs effective resistance and biharmonic distance can be estimated in time $O(m \text{ poly log } n + n^2 \text{ poly log } n)$ using an algorithm that combines Laplacian solvers and Johnson-Lindenstrauss random projection [Spielman and Srivastava, 2011].

Adding multiple edges. While the formula of Theorem 4 tells us which single edge most decreases the total resistance when added to the graph, unfortunately, we cannot use this formula to determine which set of $k \geq 2$ edges most decrease the total resistance of the graph. In Appendix B, we prove this by giving an example of a graph where the two edges that most decrease the total resistance are not the two edges that maximize the formula in Theorem 4.

We also note a challenge for designing recursive algorithms to add multiple edges: the amount an edge decreases the total resistance is ***non-monotonic*** with respect to subgraphs. By non-monotonicity, we mean that for nested graphs $H \subset G$, the amount an edge decreases the total resistance when added to G can be *more* than the amount the same edge would decrease the total resistance when added to H . Figure 3 gives an example where this is the case. Intuitively, this means that an edge can become more important to the global topology of a graph when more edges are added. This is in contrast to the effective resistance, which only decreases with the addition of more edges.

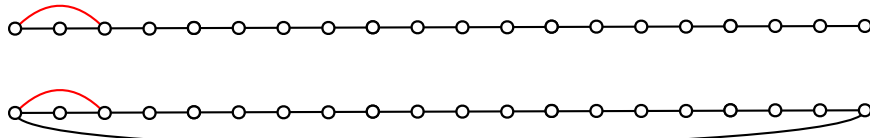
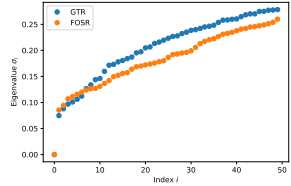


Figure 3: The path on 20 vertices is an example showing that the amount an edge decreases the total resistance is not monotonic. Top: Adding the red edge would decrease the total resistance by ≈ 30.33 . Bottom: After adding the edge connecting the first and last vertex in the path, adding the red edge would decrease the total resistance by ≈ 40.17 .

The best algorithm we know for computing the set of k edges that most decrease the total resistance is a brute-force search over all $O(\binom{n}{k})$ sets of k edges. It is reasonable to conjecture that finding the k best edges to decrease the total resistance may be hard, as the related problems of finding the k best edges to most increase the spectral gap is NP-Hard [Mosk-Aoyama, 2008]. Because of this, it is reasonable to use a heuristic rather than exactly compute the best edges to add to decrease total resistance.



	FoSR	GTR
σ_2	0.085	0.075
R_{tot}	4250377	4114024

Figure 4: A comparision of the largest connected component of Cora after adding 50 edges with FoSR and GTR. (Left) A plot of the smallest 50 eigenvalues of the Laplacian. (Right) The spectral gap and total resistance.

5 Experiments

We primarily compare our new GTR rewiring algorithm with the **FoSR** (for ‘‘first-order spectral rewiring’’) algorithm proposed by [Karhadkar et al., 2022], as FoSR is the rewiring strategy with the best performance. FoSR aims at reducing oversquashing in graphs by increasing the spectral gap. FoSR is perhaps the rewiring heuristic most similar to GTR for two reasons. First, it only changes the topology of the graph by adding edges. Second, it is designed to increase the spectral gap of the graph, which will necessarily increase the total resistance of the graph.

To compare FoSR and GTR, we use both methods to add 50 edges to the largest connected component of the Cora citation network [McCallum et al., 2000]. Figure 4 shows the 50 smallest eigenvalue after rewiring. FoSR increases the first few eigenvalues (including the spectral gap) more, while GTR increases the larger eigenvalues more. In total, GTR does more to decrease the total resistance of the graph.

5.1 Graph Classification

We evaluate our rewiring heuristic, GTR, as a preprocessing step for training a graph neural network to perform graph classification. We compare GTR with SDRF (stochastic discrete Ricci flow) from [Topping et al., 2021] as we already have compared with their results theoretically in Section 3.1. We also compare GTR with the FoSR algorithm [Karhadkar et al., 2022], which has been shown to outperform the previous rewiring algorithms DIGL [Gasteiger et al., 2019] and SRDF for graph classification. We conduct the same experiment as in [Karhadkar et al., 2022] for GTR; see Table 1 for results. We also report results for no rewiring (None), SDRF, and FoSR, all of which are taken from Table 1 of [Karhadkar et al., 2022].

Datasets. We test GTR on the same set of graph classification benchmarks as Karhadkar, Banerjee, and Montafúr. All datasets are from the TUDataset [Morris et al., 2020].

Experiments. We compare four types of graph convolutions: GCN [Kipf and Welling, 2017], Relational-GCN (R-GCN) [Battaglia et al., 2018], GIN [Xu et al., 2019], and Relational-GIN (R-GIN). Relational graph neural networks perform different aggregation steps for edges of different types. In the case of GTR, we use two edge types: original graph edges and new edges added by the rewiring algorithms.

We tune the number of edges added by GTR and fix all other hyperparameters. We use the same configuration of hyperparameters as in [Karhadkar et al., 2022]. We use randomly generated 80%/10%/10% train/validation/test splits of the data. We use the Adam optimizer and the `ReduceLROnPlateau` scheduler in Torch that reduces the learning rate after 10 epochs without an improvement in the validation accuracy. We use a stopping patience of 100 epochs of the validation loss. For the hyperparameter search, we consider average accuracies over 10 randomly generated splits of the data. For the test results, we report the average test accuracy and 95% confidence intervals over 100 randomly generated splits.

Results. Results are presented in Table 1 and the number of edges added for each graph are in Appendix C. We observe the following: (1) In general, both our GTR and FoSR outperform both the rewiring strategy SDRF or no rewiring at all. In particular, for the case of relational versions of GNNs (i.e., R-GCN and R-GIN), these two approaches often out-perform no-rewiring or SDRF by a large margin. Note that SDRF adds edges based on a local curvature criterion; while both FoSR and our GTR can add any edges, taking the global connectivity of graph into account. Table 1 shows that both two global strategies outperform the local SDRF, especially for the relation-GNN cases. (2) The performance of our GTR and FoSR are similar for the GIN and R-GIN architectures. On R-GCN however, GTR not only outperforms FoSR, but

Table 1: Results of different combinations of rewiring and convolutions on different graph classification datasets. GRT is our “Greedy Total Resistance” rewiring. FoSR is the “First-order Spectral Rewiring” rewiring of [Karhadkar et al., 2022]. SDRF is the “Stochastic Discrete Ricci Flow” rewiring of [Topping et al., 2021]. Best and second best results are reported in **blue** and **orange** respectively.

GCN						
Rewiring	Mutag	Proteins	Enzymes	Reddit-Binary	IMDB-Binary	Collab
None	72.15 ± 2.44	70.98 ± 0.74	27.67 ± 1.16	68.26 ± 1.10	49.77 ± 0.82	33.78 ± 0.49
SDRF	71.05 ± 1.87	70.92 ± 0.79	28.37 ± 1.17	68.62 ± 0.85	49.40 ± 0.90	33.45 ± 0.47
FoSR	80.00 ± 1.57	73.42 ± 0.81	25.07 ± 0.994	70.33 ± 0.72	49.66 ± 0.86	33.84 ± 0.58
GTR	79.10 ± 1.86	72.59 ± 2.48	27.52 ± 0.99	68.99 ± 0.61	49.92 ± 0.99	33.05 ± 0.40
R-GCN						
Rewiring	Mutag	Proteins	Enzymes	Reddit-Binary	IMDB-Binary	Collab
None	69.25 ± 2.09	69.52 ± 0.73	28.60 ± 1.19	49.85 ± 0.65	50.01 ± 0.92	33.60 ± 1.05
SDRF	72.30 ± 2.22	69.11 ± 0.76	33.48 ± 1.25	58.62 ± 0.65	53.64 ± 1.04	67.99 ± 0.39
FoSR	84.45 ± 1.57	73.80 ± 0.69	35.66 ± 1.151	76.59 ± 0.53	64.05 ± 1.12	70.65 ± 0.48
GTR	85.50 ± 1.47	75.78 ± 0.76	41.33 ± 1.28	80.18 ± 0.60	65.09 ± 0.93	74.34 ± 0.41
GIN						
Rewiring	Mutag	Proteins	Enzymes	Reddit-Binary	IMDB-Binary	Collab
None	77.70 ± 3.60	70.80 ± 0.83	33.80 ± 1.12	86.79 ± 1.06	70.18 ± 0.99	72.99 ± 0.38
SDRF	78.40 ± 2.80	69.81 ± 0.79	35.82 ± 1.09	86.44 ± 0.59	69.72 ± 1.15	72.96 ± 0.42
FoSR	78.00 ± 2.22	75.11 ± 0.82	29.20 ± 1.38	87.35 ± 0.60	71.21 ± 0.92	73.28 ± 0.42
GTR	77.60 ± 2.84	73.13 ± 0.69	30.57 ± 1.42	86.98 ± 0.66	71.28 ± 0.86	72.93 ± 0.42
R-GIN						
Rewiring	Mutag	Proteins	Enzymes	Reddit-Binary	IMDB-Binary	Collab
None	83.05 ± 1.44	70.50 ± 0.81	39.02 ± 1.17	87.97 ± 0.56	68.89 ± 0.87	75.54 ± 0.32
SDRF	82.70 ± 1.78	70.70 ± 0.82	39.58 ± 1.33	86.83 ± 0.52	70.21 ± 0.81	76.48 ± 0.39
FoSR	86.15 ± 1.49	74.67 ± 0.69	45.55 ± 0.13	89.67 ± 0.42	71.81 ± 0.88	76.81 ± 0.45
GTR	86.10 ± 1.76	74.44 ± 0.80	48.52 ± 1.30	89.32 ± 0.45	71.49 ± 0.93	77.35 ± 0.38

often by a reasonably large margin.

6 Concluding Remarks

In this paper, we have provided theoretical evidence that effective resistance can be used as a measure of oversquashing between a pair of nodes in a graph, and that the total resistance can be used a measure of total oversquashing in a graph. We have also empirically demonstrated that lowering total resistance improves the performance of graph neural networks.

Indeed, rewiring techniques based on total effective resistance can significantly improve performance or GNN / R-GNNs for graph classification tasks, reinforcing the notion that improving the connectivity of a graph can improve the performance of graph neural networks.

Limitations and future work. We provide theoretical evidence (Theorem 1) showing that total effective resistance can be used as a measure for the total amount of oversquashing in a graph. This is in contrast to previous work on oversquashing which relates oversquashing only to the spectral gap only intuitively. While we also show that the spectral gap can also be used as a measure for measure for oversquashing (Corollary 2), the bound for total resistance is tighter than the bound for the spectral gap.

Despite the theoretical strength of using total resistance over spectral gap for measuring oversquashing, more research is needed to contrast the effects of the two notions on oversquashing. A challenge to this task is that the total resistance and spectral gap are intimately linked; for example, adding edges to increase the spectral gap will necessarily also decrease total resistance. The oversquashing issue becomes more prominent for graphs with long range interactions (e.g., [Dwivedi et al., 2022]). Hence it will be interesting to explore a much broader family of graph benchmarks to study the pros and cons of different rewiring methods.

Finally, we also note that currently we employ a greedy approach to identify a collection of edges to be

inserted into an input graph as shortcuts. As we discussed in Section 4, it is not clear whether such greedy strategy leads to an approximation algorithm of selecting the optimal set of k edges to minimizing total effective resistance of a graph. We leave the problem of identifying efficient exact or approximate algorithms for the optimal edges for minimizing total effective resistance as a future direction to investigate.

Acknowledgements Mitchell Black and Amir Nayyeri are supported in part by NSF grants CCF-1941086 and CCF-1816442. Zhengchao Wan and Yusu Wang are supported in part by NSF Grants CCF-2217033 and CCF-2112665.

References

[Ahmad et al., 2021] Ahmad, T., Jin, L., Lin, L., and Tang, G. (2021). Skeleton-based action recognition using sparse spatio-temporal gcn with edge effective resistance. *Neurocomputing*, 423:389–398.

[Alev et al., 2018] Alev, V. L., Anari, N., Lau, L. C., and Oveis Gharan, S. (2018). Graph clustering using effective resistance. In *9th Innovations in Theoretical Computer Science Conference (ITCS 2018)*. Schloss Dagstuhl-Leibniz-Zentrum fuer Informatik.

[Alon and Yahav, 2020] Alon, U. and Yahav, E. (2020). On the bottleneck of graph neural networks and its practical implications. In *International Conference on Learning Representations*.

[Banerjee et al., 2022] Banerjee, P. K., Karhadkar, K., Wang, Y. G., Alon, U., and Montúfar, G. (2022). Oversquashing in gnns through the lens of information contraction and graph expansion. In *2022 58th Annual Allerton Conference on Communication, Control, and Computing (Allerton)*, pages 1–8.

[Battaglia et al., 2018] Battaglia, P. W., Hamrick, J. B., Bapst, V., Sanchez-Gonzalez, A., Zambaldi, V., Malinowski, M., Tacchetti, A., Raposo, D., Santoro, A., Faulkner, R., et al. (2018). Relational inductive biases, deep learning, and graph networks. *arXiv preprint arXiv:1806.01261*.

[Biggs, 1997] Biggs, N. (1997). Algebraic potential theory on graphs. *Bulletin of the London Mathematical Society*, 29(6):641–682.

[Cai and Wang, 2020] Cai, C. and Wang, Y. (2020). A note on over-smoothing for graph neural networks. *arXiv preprint arXiv:2006.13318*.

[Chandra et al., 1996] Chandra, A. K., Raghavan, P., Ruzzo, W. L., Smolensky, R., and Tiwari, P. (1996). The electrical resistance of a graph captures its commute and cover times. *computational complexity*, 6(4):312–340.

[Chung, 1996] Chung, F. R. (1996). Laplacians of graphs and cheeger’s inequalities. *Combinatorics, Paul Erdos is Eighty*, 2(157–172):13–2.

[Chung, 1997] Chung, F. R. (1997). *Spectral graph theory*, volume 92. American Mathematical Soc.

[Deac et al., 2022] Deac, A., Lackenby, M., and Veličković, P. (2022). Expander graph propagation. In *The First Learning on Graphs Conference*.

[Doyle and Snell, 1984] Doyle, P. G. and Snell, J. L. (1984). *Random walks and electric networks*, volume 22. American Mathematical Soc.

[Dwivedi et al., 2022] Dwivedi, V. P., Rampášek, L., Galkin, M., Parviz, A., Wolf, G., Luu, A. T., and Beaini, D. (2022). Long range graph benchmark. In *Thirty-sixth Conference on Neural Information Processing Systems Datasets and Benchmarks Track*.

[Gasteiger et al., 2019] Gasteiger, J., Weißenberger, S., and Günnemann, S. (2019). *Diffusion Improves Graph Learning*. Curran Associates Inc., Red Hook, NY, USA.

[Ghosh et al., 2008] Ghosh, A., Boyd, S., and Saberi, A. (2008). Minimizing effective resistance of a graph. *SIAM review*, 50(1):37–66.

[Jambulapati and Sidford, 2021] Jambulapati, A. and Sidford, A. (2021). Ultrasparse ultrasparsifiers and faster laplacian system solvers. In *Proceedings of the 2021 ACM-SIAM Symposium on Discrete Algorithms (SODA)*, pages 540–559. SIAM.

[Karhadkar et al., 2022] Karhadkar, K., Banerjee, P. K., and Montúfar, G. (2022). Fosr: First-order spectral rewiring for addressing oversquashing in gnns.

[Kipf and Welling, 2017] Kipf, T. N. and Welling, M. (2017). Semi-supervised classification with graph convolutional networks. In *International Conference on Learning Representations*.

[Kirchhoff, 1847] Kirchhoff, G. (1847). Ueber die auflösung der gleichungen, auf welche man bei der untersuchung der linearen vertheilung galvanischer ströme geführt wird. *Annalen der Physik*, 148:497–508.

[Lee et al., 2014] Lee, J. R., Gharan, S. O., and Trevisan, L. (2014). Multiway spectral partitioning and higher-order cheeger inequalities. *Journal of the ACM (JACM)*, 61(6):1–30.

[Lipman et al., 2010] Lipman, Y., Rustamov, R. M., and Funkhouser, T. A. (2010). Biharmonic distance. *ACM Trans. Graph.*, 29(3).

[Lyons and Peres, 2017] Lyons, R. and Peres, Y. (2017). *Probability on trees and networks*, volume 42. Cambridge University Press.

[McCallum et al., 2000] McCallum, A. K., Nigam, K., Rennie, J., and Seymore, K. (2000). Automating the construction of internet portals with machine learning. *Information Retrieval*, 3(2):127–163.

[Mémoli et al., 2022] Mémoli, F., Wan, Z., and Wang, Y. (2022). Persistent laplacians: Properties, algorithms and implications. *SIAM Journal on Mathematics of Data Science*, 4(2):858–884.

[Morris et al., 2020] Morris, C., Kriege, N. M., Bause, F., Kersting, K., Mutzel, P., and Neumann, M. (2020). Tudataset: A collection of benchmark datasets for learning with graphs. In *ICML 2020 Workshop on Graph Representation Learning and Beyond (GRL+ 2020)*.

[Mosk-Aoyama, 2008] Mosk-Aoyama, D. (2008). Maximum algebraic connectivity augmentation is np-hard. *Operations Research Letters*, 36(6):677–679.

[Oono and Suzuki, 2020] Oono, K. and Suzuki, T. (2020). Graph neural networks exponentially lose expressive power for node classification. In *International Conference on Learning Representations*.

[Scarselli et al., 2008] Scarselli, F., Gori, M., Tsoi, A. C., Hagenbuchner, M., and Monfardini, G. (2008). The graph neural network model. *IEEE transactions on neural networks*, 20(1):61–80.

[Spielman, 2019] Spielman, D. (2019). Spectral and algebraic graph theory. Available at <http://cs-www.cs.yale.edu/homes/spielman/sagt/sagt.pdf> (2021/12/01).

[Spielman and Srivastava, 2011] Spielman, D. A. and Srivastava, N. (2011). Graph sparsification by effective resistances. *SIAM Journal on Computing*, 40(6):1913–1926.

[Spielman and Teng, 2004] Spielman, D. A. and Teng, S.-H. (2004). Nearly-linear time algorithms for graph partitioning, graph sparsification, and solving linear systems. In *Proceedings of the Thirty-Sixth Annual ACM Symposium on Theory of Computing*, STOC '04, page 81–90, New York, NY, USA. Association for Computing Machinery.

[Topping et al., 2021] Topping, J., Di Giovanni, F., Chamberlain, B. P., Dong, X., and Bronstein, M. M. (2021). Understanding over-squashing and bottlenecks on graphs via curvature. In *International Conference on Learning Representations*.

[Xu et al., 2019] Xu, K., Hu, W., Leskovec, J., and Jegelka, S. (2019). How powerful are graph neural networks? In *International Conference on Learning Representations*.

A Proofs

A.1 Proof of Lemma 1

We will prove this using an alternative but well-known characterization of effective resistance in terms of uv -flows. First, we must define another matrix associated with a graph. Let ∂ be the $n \times m$ **boundary matrix** of the graph G , where $n := |V|$ and $m := |E|$. The matrix ∂ is defined such that for an edge $e = \{u, v\}$, the column $\partial 1_e = 1_u - 1_v$. (The order of u and v is arbitrary for what follows.)

Many of the definitions in this paper can alternatively be expressed in terms of the boundary matrix. The Laplacian can be expressed $L = \partial \partial^T$, the normalized Laplacian $\hat{L} = D^{-1/2} \partial (D^{-1/2} \partial)^T$, and the effective resistance $R_{u,v} = \min\{\|f\|^2 : \partial f = (1_u - 1_v)\}$. Phrased differently, the effective resistance between u and v is the minimum squared-2-norm of any uv -flow. This characterization of the effective resistance follows from the general fact that for any matrix AA^T and any vector $x \in \text{im } A$ we have that $x^T (AA^T)^+ x = (A^+ x)^T (A^+ x) = \min\{\|y\|^2 : Ay = x\}$. The proof of the current lemma just applies this fact twice.

$$\begin{aligned}
R_{u,v} &= (1_u - 1_v)^T L^+ (1_u - 1_v) \\
&= \min\{\|f\|^2 : \partial f = (1_u - 1_v)\} \\
&= \min\{\|f\|^2 : D^{-1/2} \partial f = D^{-1/2} (1_u - 1_v)\} \quad (\text{as } D^{-1/2} \text{ is bijective}) \\
&= \left(\frac{1}{\sqrt{d_u}} 1_u - \frac{1}{\sqrt{d_v}} 1_v \right)^T \hat{L}^+ \left(\frac{1}{\sqrt{d_u}} 1_u - \frac{1}{\sqrt{d_v}} 1_v \right).
\end{aligned}$$

A.2 Proof of Lemma 2

We prove this by induction on the layer r . For the base case of $r = 0$, either $u = v$ or $u \neq v$; in the first case

$$\frac{\partial h_u^{(0)}}{\partial x_v} = \frac{\partial x_v}{\partial x_v} = \text{Id}_{d \times d},$$

and in the second case,

$$\frac{\partial h_u^{(0)}}{\partial x_v} = \frac{\partial x_u}{\partial x_v} = 0_{d \times d}.$$

Therefore,

$$\left\| \frac{\partial h_u^{(0)}}{\partial x_v} \right\| \leq \max\{\|\text{Id}_{d \times d}\|, \|0_{d \times d}\|\} = 1. \quad (1)$$

Assume that the statement holds for some $r \geq 0$. We now prove the inductive case of $r + 1$.

$$\begin{aligned}
\left\| \frac{\partial h_u^{(r+1)}}{\partial x_v} \right\| &= \left\| \nabla_1 \phi_r \cdot \frac{\partial h_u^{(r)}}{\partial x_v} + \nabla_2 \phi_r \cdot \sum_{w \in \mathcal{N}(u)} \hat{A}_{uw} \cdot \nabla \psi_r \cdot \frac{\partial h_w^{(r)}}{\partial x_v} \right\| \\
&\leq \|\nabla_1 \phi_r\| \cdot \left\| \frac{\partial h_u^{(r)}}{\partial x_v} \right\| + \|\nabla_2 \phi_r\| \cdot \sum_{w \in \mathcal{N}(u)} \hat{A}_{uw} \|\nabla \psi_r\| \cdot \left\| \frac{\partial h_w^{(r)}}{\partial x_v} \right\| \quad (\text{as } \hat{A}_{uw} \text{ positive } \forall u, w) \\
&\leq \alpha \cdot \left\| \frac{\partial h_u^{(r)}}{\partial x_v} \right\| + \alpha \beta \cdot \sum_{w \in \mathcal{N}(u)} \hat{A}_{uw} \cdot \left\| \frac{\partial h_w^{(r)}}{\partial x_v} \right\| \\
&\leq 2^r (\alpha \beta)^{r+1} \sum_{l=0}^r (\hat{A}^l)_{uv} + 2^r (\alpha \beta)^{r+1} \sum_{l=0}^r \sum_{w \in \mathcal{N}(u)} \hat{A}_{uw} (\hat{A}^l)_{wv} \quad (\text{induction}) \\
&= 2^r (\alpha \beta)^{r+1} \sum_{l=0}^r (\hat{A}^l)_{uv} + 2^r (\alpha \beta)^{r+1} \sum_{l=1}^{r+1} (\hat{A}^l)_{uv} \quad (\text{matrix multiplication}) \\
&\leq (2\alpha\beta)^{r+1} \sum_{l=0}^{r+1} (\hat{A}^l)_{uv}.
\end{aligned}$$

Here $\nabla\phi_r = [\nabla_1\phi_r | \nabla_2\phi_r]$ and $\nabla\psi_r$ denote the Jacobian matrices for ϕ_r and ψ_r , respectively. $\nabla_1\phi_r$ corresponds to partial derivatives w.r.t. the first several arguments in ϕ_r corresponding to $h_v^{(r)}$ in the formula $\phi_r(h_v^{(r)}, \sum_{u \in \mathcal{N}(v)} \hat{A}_{uv} \psi_l(h_u^{(r)}))$ and $\nabla_2\phi_r$ is defined similarly. In the second inequality, we used the fact for 2-norm that $\|[A|B]\| \geq \max\{\|A\|, \|B\|\}$. In the third inequality, we used the fact that $\beta \geq 1$ and in this way we have that $\alpha \leq \alpha\beta$.

A.3 Proof of Theorem 1

In this section, we provide proofs of Lemma 3, Lemma 4 and Theorem 1.

Proof of Lemma 3. First, recall that the eigenvalues of \hat{A} are in the range $(-1, 1)$ if G is not bipartite. Also note that any number $\mu \in (-1, 1)$ satisfies $\sum_{j=0}^{\infty} \mu^j = \frac{1}{1-\mu}$. We prove the lemma by applying this fact to the spectral decomposition of \hat{L}^+ .

$$\begin{aligned} \hat{L}^+ &= \sum_{i=2}^n \frac{1}{\lambda_i} z_i z_i^T = \sum_{i=2}^n \frac{1}{1-\mu_i} z_i z_i^T \\ &= \sum_{i=2}^n \left(\sum_{j=0}^{\infty} \mu_i^j \right) z_i z_i^T = \sum_{j=0}^{\infty} \hat{A}_r^j. \end{aligned}$$

□

Based on Lemma 3, we then prove Lemma 4 below.

Proof of Lemma 4. Observe that

$$\begin{aligned} &\left(\frac{1}{\sqrt{d_u}} \mathbf{1}_u - \frac{1}{\sqrt{d_v}} \mathbf{1}_v \right)^T \hat{A}_r^i \left(\frac{1}{\sqrt{d_u}} \mathbf{1}_u - \frac{1}{\sqrt{d_v}} \mathbf{1}_v \right) \\ &= \left(\frac{1}{\sqrt{d_u}} \mathbf{1}_u - \frac{1}{\sqrt{d_v}} \mathbf{1}_v \right)^T \hat{A}^i \left(\frac{1}{\sqrt{d_u}} \mathbf{1}_u - \frac{1}{\sqrt{d_v}} \mathbf{1}_v \right) \end{aligned}$$

for all $i \geq 0$ as $\left(\frac{1}{\sqrt{d_u}} \mathbf{1}_u - \frac{1}{\sqrt{d_v}} \mathbf{1}_v \right)^T \mathbf{z}_1 = 0$. We use this equation to alternatively express the effective resistance.

$$\begin{aligned} R_{u,v} &= \left(\frac{1}{\sqrt{d_u}} \mathbf{1}_u - \frac{1}{\sqrt{d_v}} \mathbf{1}_v \right)^T \hat{L}^+ \left(\frac{1}{\sqrt{d_u}} \mathbf{1}_u - \frac{1}{\sqrt{d_v}} \mathbf{1}_v \right) \\ &= \sum_{i=0}^{\infty} \left(\frac{1}{\sqrt{d_u}} \mathbf{1}_u - \frac{1}{\sqrt{d_v}} \mathbf{1}_v \right)^T \hat{A}_r^i \left(\frac{1}{\sqrt{d_u}} \mathbf{1}_u - \frac{1}{\sqrt{d_v}} \mathbf{1}_v \right) \quad (\text{Lemma 3}) \\ &= \sum_{i=0}^{\infty} \left(\frac{1}{\sqrt{d_u}} \mathbf{1}_u - \frac{1}{\sqrt{d_v}} \mathbf{1}_v \right)^T \hat{A}^i \left(\frac{1}{\sqrt{d_u}} \mathbf{1}_u - \frac{1}{\sqrt{d_v}} \mathbf{1}_v \right) \quad (\text{Above observation}) \\ &= \sum_{i=0}^{\infty} \left(\frac{1}{d_u} (\hat{A}^i)_{uu} + \frac{1}{d_v} (\hat{A}^i)_{vv} - \frac{2}{\sqrt{d_u d_v}} (\hat{A}^i)_{uv} \right) \end{aligned}$$

□

Now, we finish proving Theorem 1 as follows.

Proof of Theorem 1. Now, we will combine the equation for effective resistance of Lemma 4 with the bound

on the Jacobian matrix of Lemma 2. This gives us the bound

$$\begin{aligned}
\left\| \frac{\partial h_u^{(r)}}{\partial x_v} \right\| &\leq (2\alpha\beta)^r \sum_{l=0}^r (\hat{A}^l)_{uv} \\
&\leq (2\alpha\beta)^r \cdot \frac{\sqrt{d_u d_v}}{2} \cdot \left(\frac{1}{d_u} \sum_{l=0}^{\infty} (\hat{A}^l)_{uu} + \frac{1}{d_v} \sum_{l=0}^{\infty} (\hat{A}^l)_{vv} - \frac{2}{\sqrt{d_u d_v}} \sum_{l=r+1}^{\infty} (\hat{A}^l)_{uv} - R_{u,v} \right) \\
&\leq (2\alpha\beta)^r \cdot \frac{d_{\max}}{2} \cdot \left(\frac{1}{d_u} \sum_{l=0}^{\infty} (\hat{A}^l)_{uu} + \frac{1}{d_v} \sum_{l=0}^{\infty} (\hat{A}^l)_{vv} - \frac{2}{\sqrt{d_u d_v}} \sum_{l=r+1}^{\infty} (\hat{A}^l)_{uv} - R_{u,v} \right)
\end{aligned}$$

We now simplify some of the terms in this bound. First, we partition the sums in the right-hand side of this equation as

$$\begin{aligned}
&\frac{1}{d_u} \sum_{l=0}^{\infty} (\hat{A}^l)_{uu} + \frac{1}{d_v} \sum_{l=0}^{\infty} (\hat{A}^l)_{vv} - \frac{2}{\sqrt{d_u d_v}} \sum_{l=r+1}^{\infty} (\hat{A}^l)_{uv} \\
&= \left(\frac{1}{d_u} \sum_{l=0}^r (\hat{A}^l)_{uu} + \frac{1}{d_v} \sum_{l=0}^r (\hat{A}^l)_{vv} \right) \\
&\quad + \left(\frac{1}{d_u} \sum_{l=r+1}^{\infty} (\hat{A}^l)_{uu} + \frac{1}{d_v} \sum_{l=r+1}^{\infty} (\hat{A}^l)_{vv} - \frac{2}{\sqrt{d_u d_v}} \sum_{l=r+1}^{\infty} (\hat{A}^l)_{uv} \right) \\
&= \left(\frac{1}{d_u} \sum_{l=0}^r (\hat{A}^l)_{uu} + \frac{1}{d_v} \sum_{l=0}^r (\hat{A}^l)_{vv} \right) \\
&\quad + \left(\frac{1}{\sqrt{d_u}} \mathbf{1}_u - \frac{1}{\sqrt{d_v}} \mathbf{1}_v \right)^T \sum_{l=r+1}^{\infty} \hat{A}^l \left(\frac{1}{\sqrt{d_u}} \mathbf{1}_u - \frac{1}{\sqrt{d_v}} \mathbf{1}_v \right)
\end{aligned}$$

Let $\mu = \max\{|\mu_2|, |\mu_n|\}$. We can bound the second term in the above equation using the **Courant-Fischer Theorem**, which says for a symmetric matrix B with maximum eigenvalue λ_{\max} and any vector x , one has that $x^T B x \leq x^T x \cdot \lambda_{\max}$. Then, we have that

$$\begin{aligned}
&\left(\frac{1}{\sqrt{d_u}} \mathbf{1}_u - \frac{1}{\sqrt{d_v}} \mathbf{1}_v \right)^T \sum_{l=r+1}^{\infty} \hat{A}^l \left(\frac{1}{\sqrt{d_u}} \mathbf{1}_u - \frac{1}{\sqrt{d_v}} \mathbf{1}_v \right) \\
&\leq \left(\frac{1}{d_u} + \frac{1}{d_v} \right) \sum_{r=k+1}^{\infty} \mu^r \leq \mu^{k+1} \left(\frac{1}{d_u} + \frac{1}{d_v} \right) \sum_{r=0}^{\infty} \mu^r \\
&\leq \mu^{k+1} \left(\frac{1}{d_u} + \frac{1}{d_v} \right) \frac{1}{1-\mu} \\
&\leq \mu^{k+1} \frac{2}{d_{\min}} \frac{1}{1-\mu} \tag{as $\mu \in (-1, 1)$}
\end{aligned}$$

We now bound the first term. Again, we rely on the Courant-Fischer theorem, and note that $\hat{A}_{uu}^l = \mathbf{1}_u^T \hat{A}^l \mathbf{1}_u$; however, as $\mathbf{1}_u^T \mathbf{z}_1 \neq 0$, we only get a bound of $\hat{A}_{uu}^l \leq 1 \cdot \mathbf{1}_u^T \mathbf{1}_u = 1$. Thus,

$$\frac{1}{d_u} \sum_{l=0}^r (\hat{A}^l)_{uu} + \frac{1}{d_v} \sum_{l=0}^r (\hat{A}^l)_{vv} \leq \frac{2}{d_{\min}} (r+1).$$

□

A.4 Proof of Theorem 4

In this section, we prove Theorem 4, which gives a formula for how much the effective resistance changes when an edge is added. Recall that our strategy is to apply Woodbury's formula to compute $(L + \frac{11^T}{n} + (1_u - 1_v)(1_u - 1_v)^T)^{-1}$. Before doing this, we provide a proof for Lemma 6.

Proof of Lemma 6. By Equation (7) of [Ghosh et al., 2008], one has that

$$L^+ = \left(L + \frac{11^T}{n} \right)^{-1} - \frac{11^T}{n}.$$

Then, we have that

$$(L^+)^2 = \left(L + \frac{11^T}{n} \right)^{-2} - \frac{11^T}{n} \left(L + \frac{11^T}{n} \right)^{-1} - \left(L + \frac{11^T}{n} \right)^{-1} \frac{11^T}{n} + \frac{11^T}{n}.$$

Note that vectors of the form $1_u - 1_v$ are orthogonal to the all-ones vector 1 , i.e., $(1_u - 1_v)^T 1 = 1^T (1_u - 1_v) = 0$. Hence

$$R_{u,v} = (1_u - 1_v)^T L^+ (1_u - 1_v) = (1_u - 1_v)^T (L + \frac{11^T}{n})^{-1} (1_u - 1_v),$$

and

$$B_{u,v} = (1_u - 1_v)^T (L^+)^2 (1_u - 1_v) = (1_u - 1_v)^T (L + \frac{11^T}{n})^{-2} (1_u - 1_v).$$

Now, by Theorem 3, one has that

$$R_{\text{tot}} = n \cdot \text{tr } L^+ = n \cdot \text{tr} \left(\left(L + \frac{11^T}{n} \right)^{-1} - \frac{11^T}{n} \right) = n \cdot \text{tr} \left(L + \frac{11^T}{n} \right)^{-1} - n.$$

□

Now we begin to prove Theorem 4.

Proof of Theorem 4. Adding the edge $\{u, v\}$ to G changes the Laplacian from L to $L + (1_u - 1_v)(1_u - 1_v)^T$. Then, by Lemma 6, we can find the difference in the total resistance by considering difference of $R_{\text{tot}}(G) = n \cdot \text{tr}(L + \frac{11^T}{n})^{-1} - n$ and $R_{\text{tot}}(G \cup \{u, v\}) = n \cdot \text{tr}(L + \frac{11^T}{n} + (1_u - 1_v)(1_u - 1_v)^T)^{-1} - n$. The difference of these is the trace of the third term in Woodbury's formula, which simplifies to the quantity in the statement as follows.

$$\begin{aligned} & R_{\text{tot}}(G) - R_{\text{tot}}(G \cup \{u, v\}) \\ &= n \cdot \text{tr} \left(L + \frac{11^T}{n} \right)^{-1} - n \cdot \text{tr} \left(L + \frac{11^T}{n} + (1_u - 1_v)(1_u - 1_v)^T \right)^{-1} \\ &= n \cdot \text{tr} \left(\left(1 + (1_u - 1_v)^T \left(L + \frac{11^T}{n} \right)^{-1} (1_u - 1_v) \right)^{-1} \cdot \left(\left(L + \frac{11^T}{n} \right)^{-1} (1_u - 1_v) \right) \left(\left(L + \frac{11^T}{n} \right)^{-1} (1_u - 1_v) \right)^T \right) \\ &= n \cdot \underbrace{\left(1 + (1_u - 1_v)^T \left(L + \frac{11^T}{n} \right)^{-1} (1_u - 1_v) \right)^{-1}}_I \cdot \text{tr} \left(\left(\left(L + \frac{11^T}{n} \right)^{-1} (1_u - 1_v) \right) \left(\left(L + \frac{11^T}{n} \right)^{-1} (1_u - 1_v) \right)^T \right). \end{aligned}$$

For the term I , one has that

$$\left(1 + (1_u - 1_v)^T \left(L + \frac{11^T}{n} \right)^{-1} (1_u - 1_v) \right) = (1 + R_{u,v}).$$

For the trace term, one has that

$$\begin{aligned}
& \text{tr} \left(\left(\left(L + \frac{11^T}{n} \right)^{-1} (1_u - 1_v) \right) \left(\left(L + \frac{11^T}{n} \right)^{-1} (1_u - 1_v) \right)^T \right) \\
&= (1_u - 1_v) \left(L + \frac{11^T}{n} \right)^{-2} (1_u - 1_v)^T \\
&= B_{u,v}
\end{aligned}$$

by the fact that $\text{tr}(xx^T) = x^T x$ for any vector x . \square

B Counterexample to the Greedy Algorithm.



Figure 5: The path on 5 vertices is a counterexample showing that GTR does not add the k edges that most decrease R_{tot} when $k > 1$. Left: The two edges added by GTR. GTR first adds the edge connecting the first and last vertex in the path. The total resistance of this graph is $R_{\text{tot}} \approx 8.18$. Right: The two edges that most deceases the total resistance. The total resistance of this graph is $R_{\text{tot}} \approx 7.67$.

Theorem 4 proves that GTR adds the single edge that most decreases the total resistance; however, GTR will not necessarily add the k edges that most decrease total resistance for $k > 1$. Figure 5 gives an example where this is the case.

C Experimental Details

Table 2: Number of edges added by GTR for each dataset.

GCN						
Rewiring	Mutag	Proteins	Enzymes	Reddit-Binary	IMDB-Binary	Collab
GTR	45	25	20	5	5	5
R-GCN						
Rewiring	Mutag	Proteins	Enzymes	Reddit-Binary	IMDB-Binary	Collab
GTR	50	10	40	20	40	25
GIN						
Rewiring	Mutag	Proteins	Enzymes	Reddit-Binary	IMDB-Binary	Collab
GTR	25	5	5	5	15	25
R-GIN						
Rewiring	Mutag	Proteins	Enzymes	Reddit-Binary	IMDB-Binary	Collab
GTR	15	45	45	50	20	20

Table 3: Hyperparameters for Graph Classification. These are consistent across all GNN types. These are the same as used in the experiments in [Karhadkar et al., 2022]

Hyperparameters	
Number of Hidden Layer	4
Dimension of Hidden Layers	64
Dropout	0.5
Learning Rate	1.0×10^{-3}